

Design of a Coupled BIPV/T – Solid Desiccant Cooling System for a Warm and Humid Climate

Aditya Nibandhe, Nima Bonyadi, Efstratios Rounis, Bruno Lee, Andreas Athienitis and
Ashutosh Bagchi

Department of Building, Civil and Environmental Engineering, Concordia University, Montreal
(Canada)

Abstract

The use of vapor compression systems in warm and humid climates is energy intensive due to the excessive latent load in the ambient air. As an alternative, low grade thermally driven cooling systems can contribute to lowering the cooling energy demand. The objective of this study is to investigate the performance of a solid desiccant cooling system (SDC) coupled with an air-based roof building-integrated photovoltaic/thermal (BIPV/T) system located in Chennai, India and provide the basis for the design of such a system. For this purpose, three different configurations are proposed and investigated considering the cooling performance, electrical and thermal output of the BIPV/T, desiccant regeneration temperature and thermal comfort conditions in the building. In addition, parametric studies have been conducted to further analyze the performance of each configuration. The results demonstrate that the BIPV/T outlet air temperature is maintained above 50°C for more than 40% of the daylight hours. At steady state conditions of 30°C ambient temperature, 70% RH and 60°C-80°C regeneration temperatures, supply air temperature and RH range between 25.8°C-17.1°C and 55-60% are achieved, respectively. The moisture removal capacity ranges between 1.96 gr/kg and 4.54 gr/kg for different configurations. Finally, a thermal performance (COP_{th}) of 1.81 is achieved for DINC DS configuration at regeneration temperature of 60°C.

Keywords: Solid Desiccant Cooling, BIPV/T, Energy Simulation, Warm and Humid Climate

1. Introduction

The energy consumption for space cooling applications has been doubled since 2000 and is growing faster than any other end-use in buildings due to warmer temperatures, increasing population and economic growth (IEA, 2018). Countries with hot climates might use comparatively more energy per capita than countries with moderate climate. One of the reasons for this is the higher demand for air-conditioning. Most of these countries are located near the equator, characterized by hot and warm summers (Chan, et al., 2012). Among different cooling technologies, conventional vapor compression air conditioning systems (VCS) are the most significant contributors to electricity demand and greenhouse gas emissions, especially during peak times (IEA, 2018). In extremely humid climates, an additional load is introduced by vapor compression systems (VCS), since the process air must first be cooled to its dew point and then reheated to meet thermal comfort. As an alternative, thermally driven solid desiccant cooling (SDC) can remove the moisture from the air without the additional cooling stage while benefitting from a low-grade heat source for the desiccant regeneration (Jani, et al., 2016). The fact that SDC technology is economically viable, considering the free availability of solar heat and sustainability of cooling systems, motivates further research in this area (Jani, et al., 2018).

The basic cycle of an SDC system, which comprises a rotary desiccant dehumidifier, a heater and an evaporative cooler, was first proposed by Pennington in 1955 (Pennington, 1955). Since then, several studies have been conducted by adding other components such as additional heat exchangers (Dunkle, 1965) or by combining VCS as a backup for the SDC system in high cooling demand conditions (Munters, 1968). There are also studies investigating the performance of different adsorbent materials (Asim, et al., 2019).

SDC systems provide a better control over humidity and have the advantage of desiccant regeneration at lower temperatures (60°C – 80°C) (Ge, et al., 2014) (Gommed & Grossman, 2007), (Li, et al., 2011). As a result, a source of waste heat or heat generated by a solar thermal system can be utilized for the desiccant regeneration. A combined solar assisted SDC system can be beneficial for a hot and humid climate like that of India where the peak cooling demand usually coincides with the highest levels of incident solar radiation (IEA, 2018). A development of such a system is a combination of a hybrid photovoltaic/thermal (PV/T)-SDC system, with the

added benefit of an on-site electrical generation. There are several studies investigating the utilization of solar energy as the heat source for thermally driven cooling systems. Most of these studies consider liquid-based solar thermal (PV/T) collector units (Chaudhary, et al., 2018) (Jani, et al., 2016). There are also studies considering the integration of air-based thermal collectors with SDC system. For instance, in a study by (Eicker, et al., 2010), seasonal operational performance for SDC system powered by solar air collectors is investigated. The tests have been conducted for different prototypes in Germany, China and Spain. The results show that the average seasonal COP for the German installation was close to 1.0, while this value was less for the humid climate of China. It was also reported that lower regeneration temperature with low dehumidification rates can lead to higher cooling performance.

In another classification, there are several studies that evaluate the performance of BIPV/T air collectors coupled with different air-conditioning systems for a variety of purposes and locations. Among them, Yang (Yang & Athienitis, 2016) presented a comprehensive review of major developments of various BIPV/T systems and their impact on building performance. They analysed the literature to identify vital areas of research on BIPV/T system. Shahsavari (Shahsavari & Khanmohammadi, 2019) conducted a numerical study to examine the energy and exergy performance of a BIPV/T + Thermal Wheel (TW) system and carried out a multi-objective optimization to maximize the annual obtained energy and exergy. The optimized BIPV/T+TW performs significantly better than the baseline model. This system is designed to provide pre-cooling and pre-heating for the building located in Kermanshah, Iran. Dahmane et al. (Ahmed-Dahmane, et al., 2018) designed and analyzed a BIPV/T system composed of multiple PV/T air collectors connected to an air handling unit of a building. In hot weather, the exhausted air from the building is used to decrease the PV cells temperature and increase the efficiency. They reported a maximum decrease of 9.46°C in PV cells temperature, an average increase of 0.35 in electrical efficiency in a selected day in August. However, the literature on coupled air-based building-integrated photovoltaic/thermal (BIPV/T)-SDC systems is quite limited (Infield, et al., 2006), (Buker & Riffat, 2015). Nie et al. (Nie, et al., 2017) proposed a Heat Pump assisted Solid Desiccant Cooling system (HP-SDC). They reported a maximum COP of 3.47 for the HP-SDC system which is dependent on the outdoor conditions and decreases with increase in humidity ratio. Guo et al. (Guo, et al., 2017) presented a thorough review on recent advances in PV/T heat utilization with low temperature SDC systems. It was reported that obtained outlet fluid temperature from existing PV/T systems nearly match solid desiccant cooling and dehumidification applications. They concluded that lower mass flow rate per collector area, additional glazed cover and hydraulic channel diameter optimization are important parameters that should be considered in order to achieve sufficiently high outlet fluid temperature in PV/T.

This is observed from the literature that currently there are no standard guidelines for a holistic design approach of a coupled BIPV/T-SDC system. In this study, the performance of three different configurations of a coupled air-based BIPV/T-SDC system are investigated in order to provide a basis for the design of such systems in hot and humid climates. The case study is a 50 m² retail store on the ground floor of a 4-storey building located in Chennai, India.

2. Methodology

The overall methodology followed in this investigation includes the following steps:

First, the cooling load of the retail store (conditioned space) is estimated through energy simulation. In the second step, the model of base case cooling cycle with BIPV/T system is developed to maintain the cooling load. Next, different configurations of SDC cycles are modeled and parametric analysis for the various components' operation in each configuration is performed. All the configurations are simulated at steady state conditions of 30°C temperature and 70% relative humidity. The objective is to achieve lower supply and regeneration air temperatures while maintaining a relatively low system complexity. In the last step, the optimal regeneration flow rates are assigned as constraints for the improvement of the BIPV/T system. Based on these results, the optimum operation conditions of the BIPV/T system are obtained. In addition, the useful heat delivered for the regeneration of the desiccant wheel is maximized while maintaining PV temperatures below 75°C.

2.1. Cooling energy demand estimation

A 4-storey mixed-use residential building in Chennai, India is selected for this study. There are two retail stores 50 m² each and parking on the ground floor. Each floor consists of two 55 m² and two 45 m² residential units. The

building envelope and ventilation rates for the retail store are designed according to the Indian building codes. This is a typical building which represents the current residential building stock in India. A 50 m² retail store located on the ground floor of the residential building is simulated. The cooling schedule of the retail store is set based on the working hours which is between 10 AM to 5 PM. The annual cooling energy demand for the retail store is approximately 4,100 kWh with sensible to latent heat ratio of 0.70.

2.2. Energy modelling and simulations

The building geometry is modelled using TRNSYS 3D plugin in SketchUp Make 2017. The building energy model as well as the coupled BIPV/T + SDC system is developed in TRNSYS 18. TRNSYS component Type 56 is used to model the multi-zone building. The results of the simulated data of the building's annual energy profile is compared with surveyed data of similar residential building stock in Chennai, India. The comparison shows that results of simulated data is within acceptable range of the surveyed data. The BIPV/T component is modelled using type 569 with some minor modifications to conform to the actual system used for experimental study. The results of simulated data for outlet temperature from BIPV/T is compared with the measured data taken from the experimental setup. The comparison shows that results of simulated data is within acceptable range of the experimental data. All the important components used in TRNSYS are listed in the Table 1.

Table 1. TRNSYS model components

Sr. No.	Type	Description
1	Type 14, type 41	Forcing function for schedule set
2	Type 56	Multi-zone building
3	Type 569, type 566	Un-glazed BIPV and glazed BIPV for BIPV/T component
4	Type 716	Rotary desiccant dehumidifier
5	Type 760	Sensible air-to-air heat recovery wheel
6	Type 663	Unit heater
7	Type 507	Evaporative cooling device
8	Type 642	Single speed fan/blower

2.3. BIPV/T system

The rendering of the roof BIPV/T system is shown in Figure 1. The available rooftop area for the BIPV/T application is approximately 220 m². The structure of the BIPV/T system is lightweight framing with simple attachment methods at the roof. The tilt of 13° is set as the optimal collector angle for Chennai. Two set of BIPV/T systems with 42 and 49 modules are considered as shown in Figure 1.

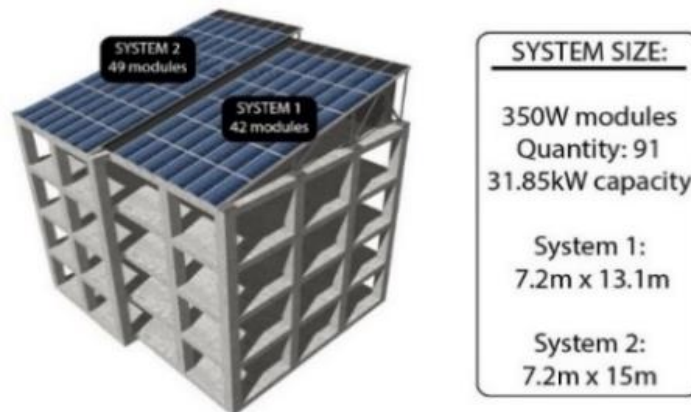


Figure 1. Rendering of the roof BIPV/T system

2.4. SDC configurations

Two Different configurations are proposed in this study to improve the performance of the coupled BIPV/T-SDC system. The Direct-Indirect Evaporative Cooling (DINC) cycle shown in Figure 2 has the advantages of simplicity and comparatively higher thermal COP (Jani, et al., 2016). The cooling cycle consists of a Desiccant Wheel (DW), a Sensible Wheel (SW), an Auxiliary Heater (AH) coupled with a BIPV/T system, and combination of Indirect Evaporative Cooler (IEC) and Direct Evaporative Cooler (DEC). In the DINC cycle, part of the return air is used as a secondary stream in the IEC and the remaining part is mixed with the supply air coming out of the sensible wheel.

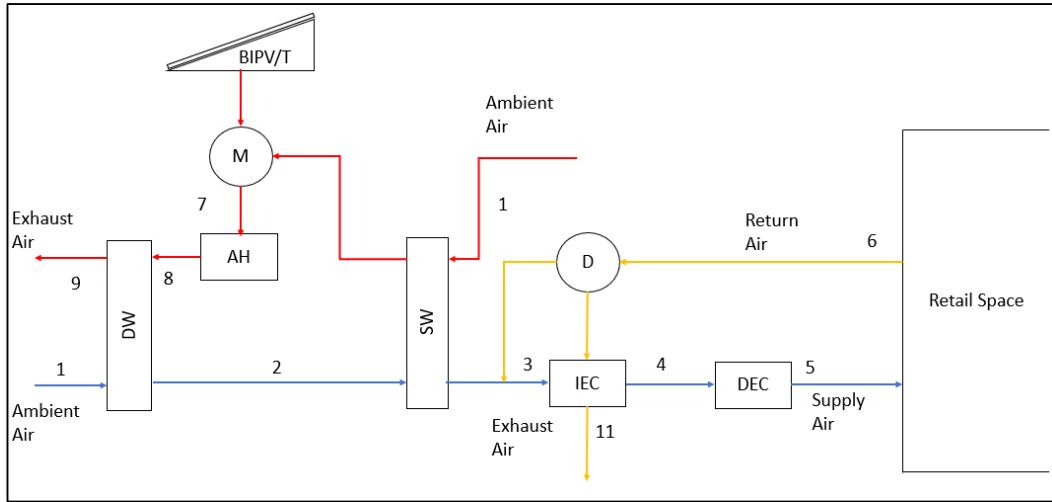


Figure 2. Base case model (DINC) configuration

The DINC cycle is considered as the base case model. Two other modified configurations, DINC-D and DINC-DS, are also developed to improve the base case model with the goal of reducing supply air temperatures at the inlet of the conditioned space and incoming ambient air at the inlet of the desiccant wheel. In the first modified configuration (DINC-D) shown in Figure 3, another direct evaporative cooler is added right after the diverter. This modification decreases the temperature at this point of the return air stream that passes through the sensible wheel. Thus, no additional ambient air is required to be introduced at the inlet of the sensible wheel. Furthermore, this modification in the process enhances the indoor air quality as opposed to the basic DINC cycle, where a large portion of the return air is mixed with the supply air.

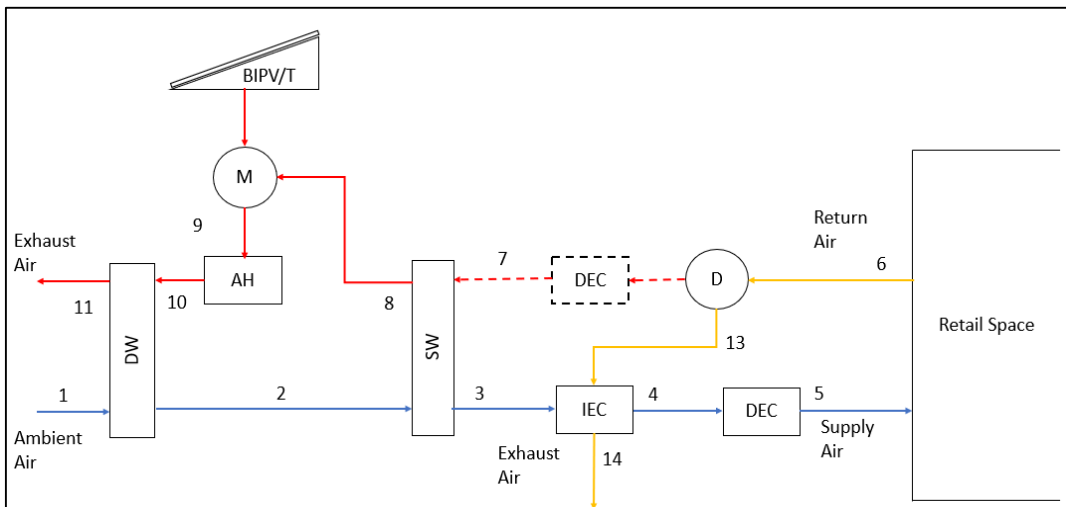


Figure 3. Configuration DINC-D

In the second modified configuration (DINC-DS) shown in Figure 4, in addition to the changes made in DINC-D, another diverter and a sensible wheel are added to the cycle. The return air coming out of the direct evaporative cooler introduced in DINC-D gets further split into two air streams. One of these streams is introduced to the first sensible wheel which is part of the basic cycle and the other air stream is introduced to the newly added sensible wheel (SW II). The second sensible wheel is placed before the desiccant wheel, in order to reduce the temperature of incoming ambient air at the inlet of the desiccant wheel.

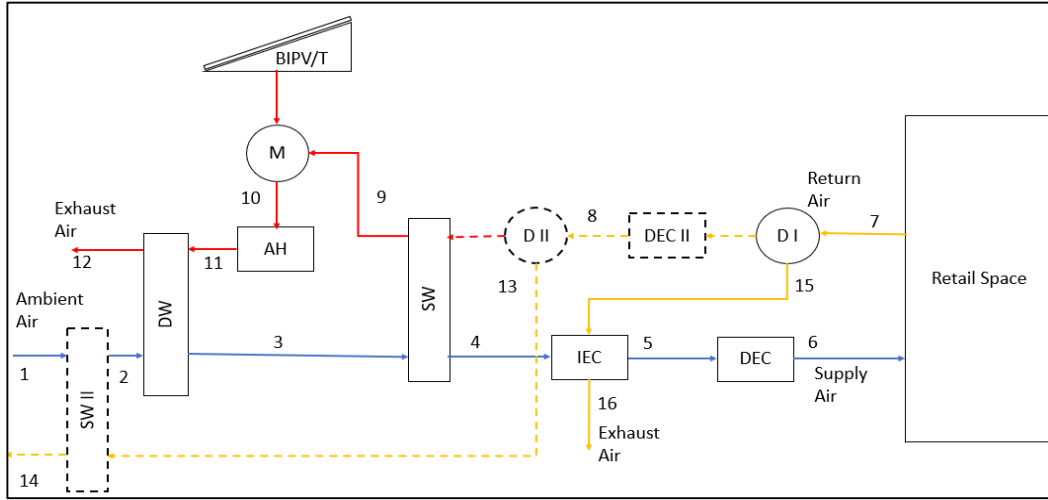


Figure 4. Configuration DINC-DS

2.5. Thermal COP of the cooling system

In this study, the following indices are considered to analyze the performance of the system.

First, the thermal coefficient of performance (COP_{th}) of the system is calculated using equation 1. Ambient air is used to supply fresh air to the building. Therefore, the enthalpy difference between ambient air and room supply air is considered as useful cooling energy. On the other hand, the heat required for regeneration is calculated by the enthalpy difference between regeneration air in the desiccant wheel inlet and enthalpy at the heat exchanger inlet. Accordingly, the COP_{th} of the system is calculated and reported for different configurations.

$$COP_{th} = \frac{q_{cool}}{q_{heat}} = \frac{\dot{m}_{supply}(h_{amb} - h_{supply})}{\dot{m}_{return}(h_{reg} - h_{HX})} \quad (\text{eq. 1})$$

Second, the moisture removal capacity (MRC) (gr/kg) is used to determine the amount of water content that is removed from the incoming ambient air before it is processed further in the cycle and supplied. The moisture removal capacity of the desiccant wheel is determined by considering the humidity ratio (moisture content) of the incoming ambient air and outgoing process air from the desiccant wheel (Enteria, et al., 2010).

$$MRC = \dot{m}_{process}(w_{amb} - w_{process\ DW\ out}) \quad (\text{eq. 2})$$

Lastly, the dehumidification efficiency (η_{deh}) is calculated as the ratio of dehumidification reached in the desiccant wheel to the theoretical possible dehumidification (Eicker, et al., 2012). The ideal specific humidity (w_{ideal}) is taken as zero by assuming that the air is completely dehumidified at the exit of the desiccant wheel.

$$\eta_{deh} = \frac{(w_{amb} - w_{process\ DW\ out})}{(w_{amb} - w_{ideal})} \quad (\text{eq. 3})$$

3. Results and discussions

3.1. BIPV/T results

The simulated annual BIPV/T system performance is shown in Figure 5. Outlet air temperatures over 50°C can be reached for approximately 40% of the daylight hours and thus help to significantly reduce the required heating energy demand for the desiccant regeneration. The annual electrical and thermal output of the system is expected to be around 20 MWh and 22 MWh, respectively.

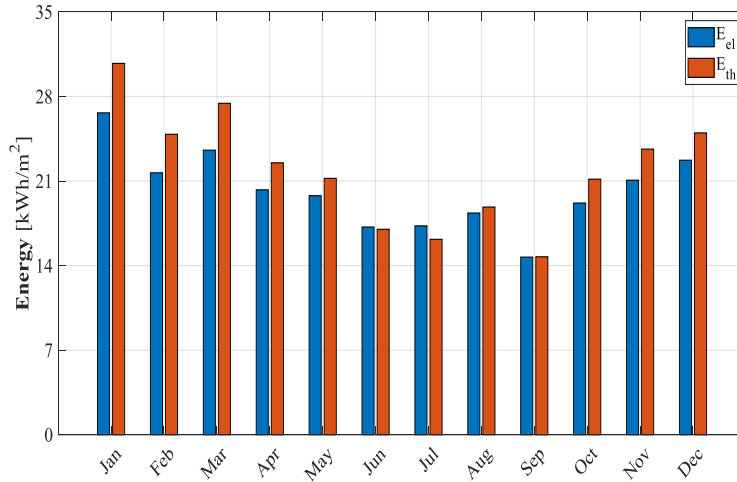


Figure 5. Results for simulated annual BIPV/T system performance

3.2. Psychrometric charts

Figure 6.a presents the psychrometric chart of DINC cycle at the steady state condition. The process air cycle (states 1-6) is shown in blue color. In DINC cycle, ambient air (process air) enters the system at state 1 and undergoes dehumidification in the desiccant wheel until state 2. Next, the process air is further sensibly cooled first by sensible wheel until state 3 and then by the indirect evaporative cooler until state 4. Then, the process air goes through an evaporative cooling process in the direct evaporative cooler until state 5 at which point it is supplied to the retail store. The supplied air absorbs heat from the retail store and reaches state 6. The regeneration cycle (states 1-9) is shown in red color. The ambient air is taken into the sensible wheel and sensibly heated to state 7. At this state, heated ambient air at the sensible wheel exit is mixed with heated ambient air coming from the BIPV/T system. Since both the sensible wheel and BIPV/T use ambient air, the humidity ratio of the regeneration air does not change. This mixture undergoes further sensible heating in the auxiliary heater to reach the setpoint regeneration temperature of 70°C. Finally, the regeneration air enters the desiccant wheel wherein it desorbs the desiccant wheel and exits at state 9.

In case of DINC-D, shown in Figure 6.b, the return air from the retail store at state 6 is cooled and humidified using a secondary direct evaporative cooler until state 7. From states 7-8, the return air follows the same sensible heating process through the sensible wheel as DINC cycle. At state 8, the return air from the sensible wheel is mixed with outgoing heated ambient air from the BIPV/T which is at a slightly higher temperature and humidity ratio. At state 9, the return air temperature is increased by sensible heating in the auxiliary heater until it reaches state 10. At this state, desorption process starts in the desiccant wheel and the return air exits at state 11. Since return air from the retail store is used as a part of the regeneration air, the humidity ratio in DINC-D is lower than DINC cycle.

In DINC-DS, shown in Figure 6.c, an additional sensible wheel is introduced at the beginning of the process air cycle. The sensible wheel sensibly cools the incoming ambient air before it enters the desiccant wheel. In this way, the desiccant wheel performance is improved and supply air temperature to the retail store is reduced. In the regeneration cycle, the outgoing heated ambient air from the BIPV/T is mixed with the return air exiting from the sensible wheel (states 9-10). At state 10, although the humidity ratio of the regeneration air increases slightly, the regenerating air temperature is increased by 2-3°C. In regular operation, it can boost up to a higher temperature resulting in lower required regeneration heat (Q_{Reg}) and higher COP_{th} .

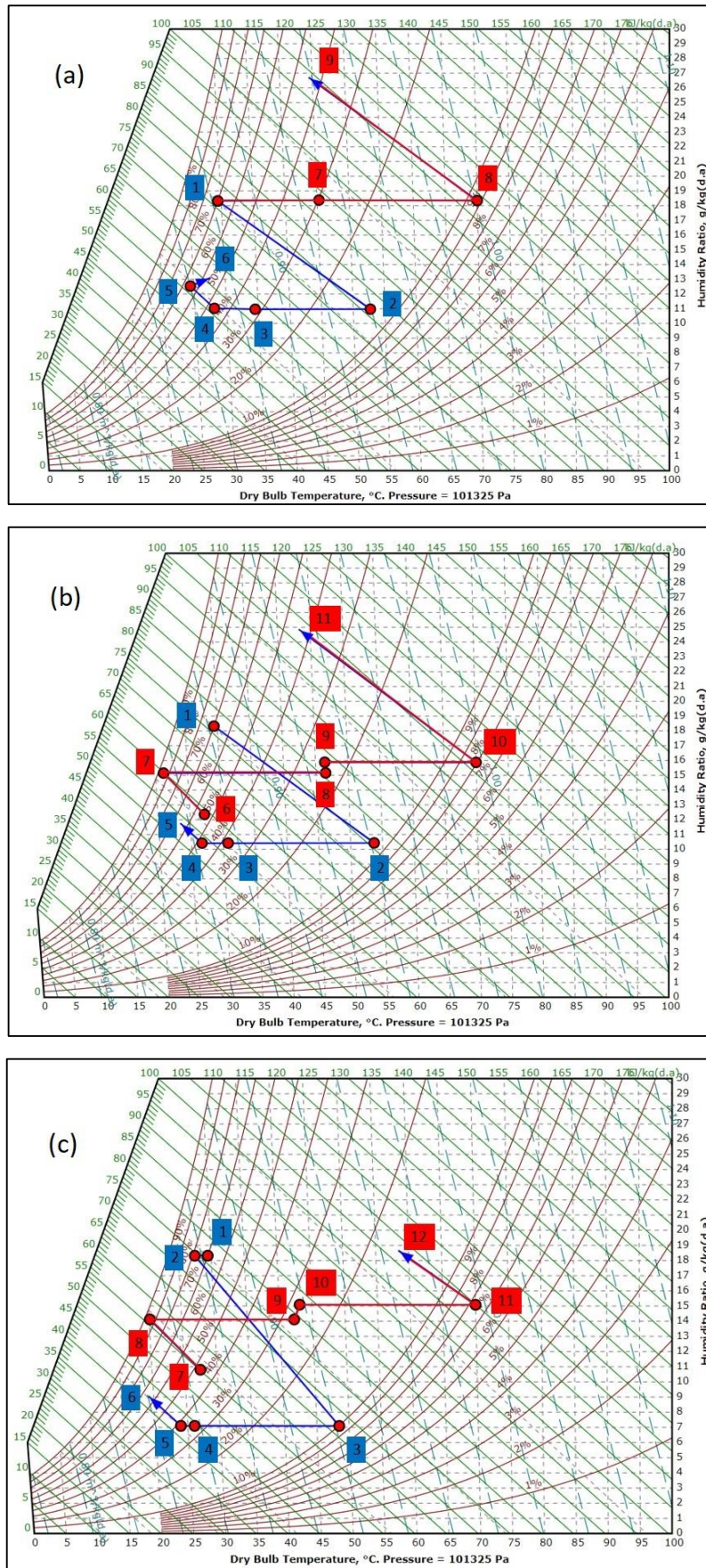


Figure 6. Psychrometric charts for different configurations: a) DINC, b) DINC-D, c) DINC-DS

3.3. Parametric analysis

All the simulations were carried out at 30°C and 70% RH with regeneration temperatures from 60°C to 80°C. The moisture removal capacity ranges between 1.96 gr/kg (DINC) and 4.54 gr/kg (DINC-DS). The dehumidification efficiency (η_{deh}) of a desiccant wheel is an effective metric to determine its performance. The dehumidification efficiency of the desiccant wheel increases with higher regeneration temperature (T_{Regen}). As shown in Figure 7, at regeneration temperature of 60°C, moisture removal capacity for the desiccant wheel in DINC cycle is 1.96 gr/kg and the dehumidification efficiency is 31%. By contrast, at regeneration temperature of 80°C, moisture removal capacity for the same case is 3.07 gr/kg with a higher dehumidification efficiency of 48%. However, dehumidification efficiency can be the same for different cases at different conditions. For example, the dehumidification efficiency for DINC at T_{Regen} of 80°C and DINC-DS at regeneration temperature of 60°C is 48%. In this case, lower process air temperature at the desiccant wheel exit will result at lower supply air temperature. The DINC-DS has lower process air temperature at the desiccant wheel exit and consequently lower supply air temperature as well. Therefore, the desiccant wheel in DINC-DS can achieve better moisture removal capacity performance than DINC.

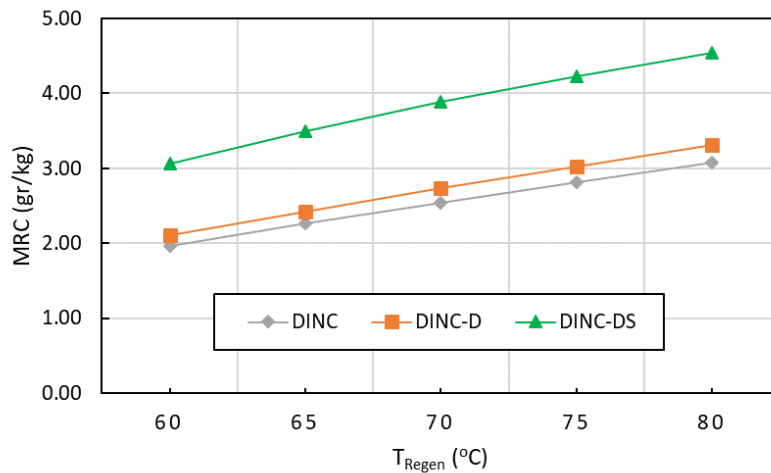


Figure 7. MRC variation with regeneration temperature for different configurations

As shown in Figure 8, the supply air temperatures in the DINC cycle is in the range of 25.9°C-23.1°C. The configurations DINC-D and DINC-DS achieved supply air temperatures as low as 21.8°C and 17.1°C respectively. The desiccant wheel performance decreases when incoming ambient air temperature increases. The introduction of a second sensible wheel before the process air inlet to desiccant wheel in the DINC-DS, reduces the ambient air temperature without changing the moisture content. This modification results in a lower process air temperature at the exit of desiccant wheel, further improving the supply air temperature.

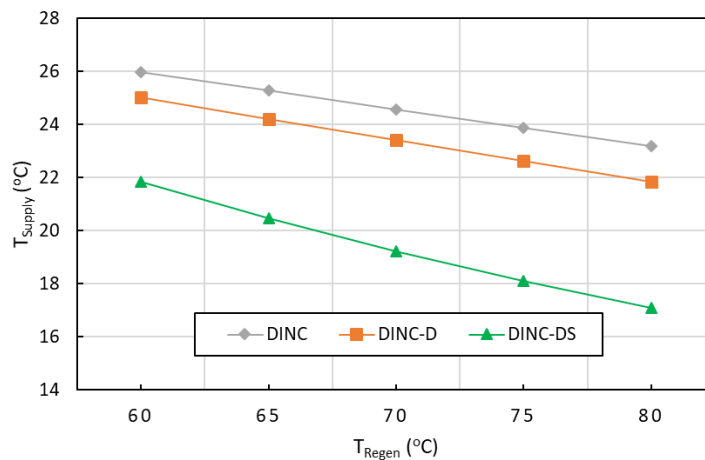


Figure 8. Supply air temperature variation with regeneration temperature for different configurations

The variation of temperature and humidity ratio of air at the outlet of the desiccant wheel with different regeneration temperature is shown in Figure 9. As illustrated, the outlet air has both lower temperature and humidity ratio in DINC-DS cycle in comparison to the DINC cycle. Also, applying higher regeneration temperature increases the outlet temperature and decreases the humidity ratio of the air passing through the desiccant wheel.

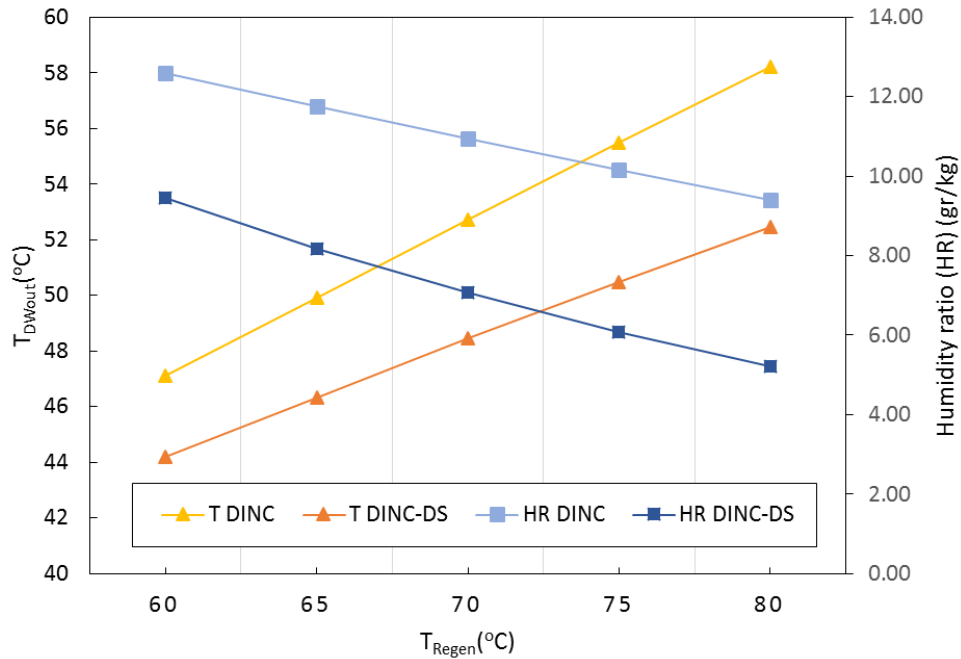


Figure 9. DW outlet temperature and HR variations with regeneration temperature for different configurations

As shown in Figure 10, the lowest COP_{th} of 0.89 at regeneration temperature of 80°C is achieved by the system using the DINC cycle whereas the highest COP_{th} of 1.81 at regeneration temperature of 60°C is achieved for the DINC-DS. The SDC system in the DINC cycle uses fresh ambient air at the inlet of sensible wheel. This results in higher enthalpy at the exit of the sensible wheel which in turn increases the regeneration heat. On the other hand, for system using DINC-D or DINC-DS, return air from the room is recirculated to sensible wheel resulting lower enthalpy at the exit as compared to DINC cycle. In this way, these systems achieve higher COP_{th} . It should also be noted that lower regeneration temperature means lower regeneration enthalpy and consequently lower regeneration heat.

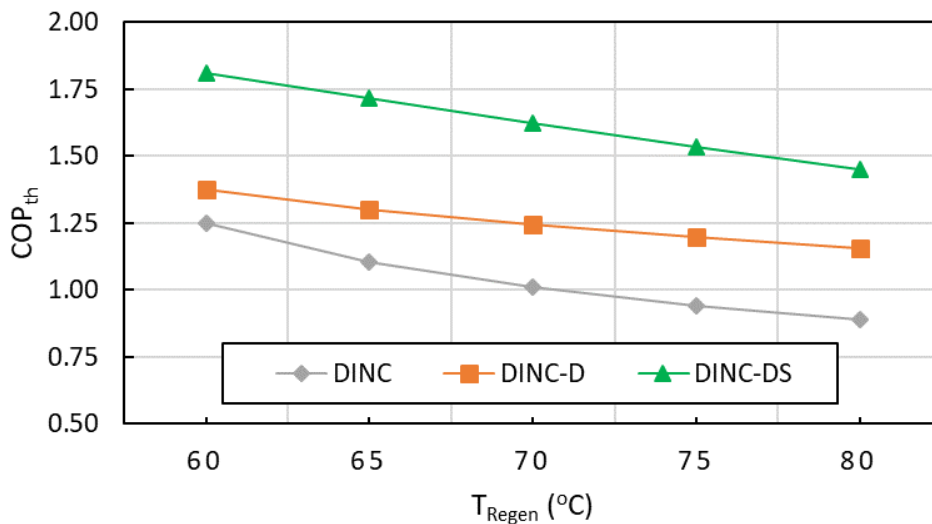


Figure 10. Thermal COP variation of SDC system with regeneration temperature for different configurations

In case the SDC system cannot maintain the thermal comfort, conventional VCS systems such as a split-type AC can be deployed together with the SDC to fulfill the cooling demand throughout the year. The hybrid system will significantly reduce the size of the VCS system.

4. Conclusions

The results of this study show that there is a considerable potential for a coupled air based BIPV/T - SDC system for warm and humid climates. In this study, the Direct Indirect Evaporative Cooling (DINC) cycle is taken as the base case and two new modifications are introduced without adding complexity to the existing cycle. The Direct Indirect Evaporative Cooling cycle with additional Direct Evaporative Cooler and Sensible Wheel (DINC-DS) achieves the highest thermal Coefficient of Performance of 1.81, highest Moisture Removal Capacity of 4.54 gr/kg and lowest supply air temperature of 17.1°C compared to the other two cycles. The DINC-DS achieves significantly better performance in comparison with the DINC-D, although it uses an extra sensible wheel. This performance improvement is primarily because of higher Moisture Removal Capacity (MRC) in DINC-DS. Also, recirculation of return air for regeneration in the DINC-D and the DINC-DS helps to maintain lower humidity ratio in the supply air in comparison with the DINC. This aids in the evaporative cooling process and cools the air even further. From this study, it can be concluded that the coupling of a BIPV/T collector and SDC system improves the overall performance of the system.

In this study, the performance indices of the system (COP_{th} , MRC, and η_{deh}) are analysed by considering regeneration temperature, regeneration heat, and supply air temperature as design parameters. There are also other important parameters such as mass flow rates and energy consumption by the individual components of the system which will be addressed in the future work. As a part of the future work, a multi-objective optimization study will be conducted to improve the performance of the coupled system. The focus of the future work will be on maximizing the BIPV/T outlet air temperature and minimizing the energy consumption of the coupled system.

5. Acknowledgements

The authors gratefully acknowledge the financial support provided by the India-Canada Centre for Innovative Multidisciplinary Partnerships to Accelerate Community Transformation and Sustainability (IC-IMPACTS).

6. References

- Ahmed-Dahmane, M., Malek, A. & Zitoun, T., 2018. Design and analysis of a BIPV/T system with two applications controlled by an air handling unit. *Energy Conversion and Management*, Volume 175, pp. 49-66.
- Asim, N. et al., 2019. Key factors of desiccant-based cooling systems: Materials. *Applied Thermal Engineering*.
- Buker, M. & Riffat, S., 2015. Building integrated solar thermal collectors - A review.. *Renew. Sustain. Energy Rev.*, Volume 51, p. 327-346.
- Chan, H. Y., Zhu, J. & Riffat, S., 2012. Solar facade for space cooling. *Energy and Buildings*, pp. 307-319.
- Chaudhary, G. et al., 2018. Integration of solar assisted solid desiccant cooling system with efficient evaporative cooling technique for separate load handling. *Applied Thermal Engineering*, pp. 696-706.
- Dunkle, R., 1965. A method of solar air conditioning. 73(73-8).
- Eicker, U. et al., 2010. Operational experiences with solar air collector driven desiccant cooling systems. *Applied Energy*, pp. 3735-3747.
- Eicker, U. et al., 2012. Experimental investigations on desiccant wheels. *Applied Thermal Engineering*, pp. 71-80.
- Enteria, N. et al., 2010. Experimental heat and mass transfer of the separated and coupled rotating desiccant wheel and heat wheel. *Experimental Thermal and Fluid Science*, pp. 603-615.
- Ge, T., Dai, Y. & Wang, R., 2014. Review on solar powered rotary desiccant wheel cooling system. *Renewable and Sustainable Energy Reviews*, pp. 476-497.

Gommed, K. & Grossman, G., 2007. Experimental investigation of a liquid desiccant system for solar cooling and dehumidification. *Solar Energy*, 81(1), pp. 131-138.

Guo, J. et al., 2017. A review of photovoltaic thermal (PV/T) heat utilisation with low temperature desiccant cooling and dehumidification. *Renewable and Sustainable Energy Reviews*, Volume 67, pp. 1-14.

IEA, 2018. *The Future of Cooling*. s.l.:s.n.

Infield, D. G., Eicker, U., Fux, V. M. L. & Schumacher, J., 2006. A simplified approach to thermal performance calculation for building integrated mechanically ventilated PV facades. *Building and Environment*, 41(7), pp. 893 - 901.

Jani, D. B., Mishra, M. & Sahoo, P., 2018. A critical review on application of solar energy as renewable regeneration heat source in solid desiccant – vapor compression hybrid cooling system. *Journal of Building Engineering*, pp. 107-124.

Jani, D., Mishra, M. & Sahoo, P., 2016. Solid desiccant air conditioning - A state of the art review. 60(1451-1469).

Li, H. et al., 2011. Experimental investigation on a one-rotor two-stage desiccant cooling/heating system driven by solar air collectors.. *Appl. Therm. Eng.*, Volume 31, p. 3677–3683.

Munters, C., 1968. *Inorganic, fibrous, gas-conditioning packing for heat and moisture transfer*. United States, Patent No. 3, 377, 225.

Nie, J. et al., 2017. Theoretical modelling and experimental study of air thermal conditioning process of a heat pump assisted solid desiccant cooling system. *Energy and Buildings*, pp. 31-40.

Pennington, N., 1955. *Humidity changer for air conditioning*. United States, Patent No. 2, 700, 537.

Shahsavari, A. & Khanmohammadi, S., 2019. Feasibility of a hybrid BIPV/T and thermal wheel system for exhaust air heat recovery: Energy and exergy assessment and multi-objective optimization. *Applied Thermal Engineering*, Volume 146.

Yang, T. & Athienitis, A., 2016. A review of research and developments of building-integrated photovoltaic/thermal (BIPV/T) systems. *Renewable and Sustainable Energy Reviews*, Volume 66, pp. 886-912.